Since January 2020 Elsevier has created a COVID-19 resource centre with free information in English and Mandarin on the novel coronavirus COVID-19. The COVID-19 resource centre is hosted on Elsevier Connect, the company's public news and information website.

Antiviral Research 207 (2022) 105419

Contents lists available at ScienceDirect

Antiviral Research

journal homepage: www.elsevier.com/locate/antiviral

Repurposing of HIV/HCV protease inhibitors against SARS-CoV-2 3CL^{pro}

Ling Ma [a,1], Quanjie Li [a,1], Yongli Xie [a,1], jianyuan Zhao [a], Dongrong Yi [a], Saisai Guo [a], Fei Guo [b], Jing Wang [a,**], Long Yang [c,***], Shan Cen [a,*]

[a] Institute of Medicinal Biotechnology, Chinese Academy of Medical Science, Beijing, China
[b] Institute of Pathogen Biology, Chinese Academy of Medical Science, Beijing, China
[c] School of Integrative Medicine, Tianjin University of Traditional Chinese Medicine, Tianjin, 301617, China

ARTICLE INFO

Keywords:
Severe acute respiratory syndrome coronavirus 2
Anti-coronavirus drug
Screening assay
Protease

ABSTRACT

Severe acute respiratory syndrome coronavirus 2 (SARS-CoV-2) is the pathogen that caused the global COVID-19 outbreak. The 3C-like protease (3CL^{pro}) of SARS-CoV-2 plays a key role in virus replication and has become an ideal target for antiviral drug design. In this work, we have employed bioluminescence resonance energy transfer (BRET) technology to establish a cell-based assay for screening inhibitors against SARS-CoV-2 3CL^{pro}, and then applied the assay to screen a collection of known HIV/HCV protease inhibitors. Our results showed that the assay is capable of quantification of the cleavage efficiency of 3CL^{pro} with good reproducibility (Z′ factor is 0.59). Using the assay, we found that 9 of 26 protease inhibitors effectively inhibited the activity of SARS-CoV-2 3CL^{pro} in a dose-dependent manner. Among them, four compounds exhibited the ability to bind to 3CL^{pro} *in vitro*. HCV protease inhibitor simeprevir showed the most potency against 3CL^{pro} with an EC_{50} vale of 2.6 μM, bound to the active site pocket of 3CL^{pro} in a predicted model, and importantly, exhibited a similar activity against the protease containing the mutations P132H in Omicron variants. Taken together, this work demonstrates the feasibility of using the cell-based BRET assay for screening 3CL^{pro} inhibitors and supports the potential of simeprevir for the development of 3CL^{pro} inhibitors.

1. Introduction

The recent outbreak of a novel coronavirus disease (COVID-19), which caused severe acute respiratory (SAR) symptoms, has spread rapidly worldwide and led to over 258 million confirmed cases with a ~2% case fatality rate as of Nov 24, 2021 (World Health Organization). The etiological agent responsible for the global pandemic is a new coronavirus (CoV), named severe acute respiratory syndrome coronavirus 2 (SARS-CoV-2), which shares about 80% of RNA genome identity with SARS-CoV. Currently, several COVID-19 vaccines have been made significant development (Sciscent et al., 2021), and a total of 10 drugs have been approved by Food and Drug Administration (FDA) or granted emergency use authorization (EUA) (FDA US, 2019). Especially, the recent rises of several high transmissible variants including Delta and Omicron strains of SARS-CoV-2 sounded alarms for currently used vaccines and neutralizing antibodies. Thus, there is still an urgent need to develop effective measure not only against this highly pathogenic virus but also for protection from future viral outbreaks.

SARS-CoV-2 contains an enveloped, positive-sense, single-stranded RNA that is ~30,000 nt in length, and its replicase gene encodes two overlapping polyproteins, pp1a and pp1ab. The SARS Chymotrypsin-like cysteine protease (3CL^{pro}), also referred to as the main protease (M^{pro}), is the primary enzyme responsible for proteolysis (Cannalire et al., 2020). The sequence alignment shows that SARS-CoV-2 3CL^{pro} is about 96% and 50% identical to SARS-CoV and MERS-CoV main proteases, respectively, which also reveals structural similarity of 3CL^{pro} among the three CoVs (Sciscent et al., 2021; Mirza and Froeyen, 2020; Cao et al., 2020). The 3CL^{pro} prefers to recognize the substrates involving the Leu-Gln↓(Ser, Ala, Gly) sequence and no human protease with the similar cleavage specificity is known. Along with the papain-like protease(s), this enzyme cleaves the polyproteins at no less than 11 sites into 16 nonstructural functional proteins (nsp1 to nsp16)

* Corresponding author.
** Corresponding author.
*** Corresponding author.
E-mail addresses: jingwang@imb.pumc.edu.cn (J. Wang), longyangrich@hotmail.com (L. Yang), shancen@imb.pumc.edu.cn (S. Cen).
[1] These authors contributed equally to this work.

https://doi.org/10.1016/j.antiviral.2022.105419
Received 7 June 2022; Received in revised form 18 August 2022; Accepted 12 September 2022
Available online 23 September 2022

(Mengist et al., 2020; Zhang et al., 2020). These nsps are mainly involved in viral replication and production of sub-genomic mRNA that encode four structural proteins-spike (S), nucleocapsid (N), membrane (M) and envelop (E), and other accessory proteins. Therefore, $3CL^{pro}$ plays an important role in maturation of SARS-CoV-2, and inhibition of the activity of $3CL^{pro}$ is expected to block the viral replication. Overall, the conservation features of $3CL^{pro}$ and its functional importance in the viral life cycle have turned it into an attractive antiviral target for the development of broad-spectrum, less-toxicity and effective drugs.

To present, several studies have been reported to identify the potential inhibitors targeting the $3CL^{pro}$ of SARS-CoV-2. The oral SARS-CoV-2 $3CL^{pro}$ inhibitor nirmatrelvir has been approved by the FDA in combined use with ritonavir (Paxlovid) for Covid 19 treatment (Owen et al., 2021; Ahmad et al., 2021; Yang et al., 2022). Also, there are several other drug candidates targeting SARS-CoV-2 $3CL^{pro}$ in clinical trials, such as lopinavir, Darunavir, ASC09 and Danoprevir (Lee and Kim, 2022; BioRender). A combination of two HIV-1 protease inhibitors lopinavir/ritonavir (Kaletra) have been used for possible treatment of COVID-19. The study of molecular complexation between each inhibitor and SARS-CoV-2 $3CL^{pro}$ indicated that both drugs interact well with the residues at the active site of SARS-CoV-2 $3CL^{pro}$ (Nutho et al., 2020). However, a trial of lopinavir/ritonavir treatment in hospitalized adults with severe COVID-19 showed that the curative effect remains very limited (Cao et al., 2020). Recently, several crystal structures of the unliganded SARS-CoV-2 $3CL^{pro}$ and its complex with inhibitors have been resolved (Zhang et al., 2020; Jin et al., 2020; Dai et al., 2020). The studies have suggested that these compounds N3 and ebselen (Jin et al., 2020), 11a and 11b (Dai et al., 2020), and improved α-ketoamide inhibitors (Zhang et al., 2020) show the potential to develop as promising drug candidates against COVID-19. The availability of the crystal structure of SARS-CoV-2 $3CL^{pro}$ also promotes many initial computational studies to screen compounds or existing drugs against COVID-19 (Sk et al., 2020; Lobo-Galo et al., 2020; Khan et al., 2020; Islam et al., 2020; Ton et al., 2020; Kandeel and Al-Nazawi, 2020). However, many of these candidates with inhibitory effects still need to be further confirmed by *in vitro* and *in vivo* experiments.

In this study, in order to facilitate the rapid discovery of potent $3CL^{pro}$ inhibitors as SARS-CoV-2 antivirals, we developed the cell-based, bioluminescence resonance energy transfer (BRET) assay for the SARS-CoV-2 $3CL^{pro}$ inhibitor screening and exploited it to screen a set of protease inhibitors, with the expectation of repurposing candidates against SARS-CoV-2 $3CL^{pro}$.

2. Materials and methods

2.1. Cell culture and transfection

HEK293T cells were maintained in Dulbecco's modified Eagle's medium (DMEM, Gibco) supplemented with 10% fetal bovine serum (FBS, Gibco) and 1% penicillin-streptomycin solution (Invitrogen) at 37 °C and 5% CO_2. For cell transfection, cells were plated at a density of 2×10^5 cells/ml. After 24 h incubation, cells were transfected using Lipofectamine 2000 (Invitrogen) according to the manufacturer's instructions.

2.2. Plasmid, antibodies and reagents

The pEYFP-linker-Rluc expression construct was generated by PCR using the pEYFP-N1 (Clontech) as template, with the designed primers harboring $3CL^{pro}$ recognition sequence (linker: ITSAVLQSGFRK). The PCR amplified EYFP-linker fragment was then inserted into the pRLuc-N2 expression construct (PerkinElmer). The full-length gene encoding SARS-CoV-2 $3CL^{pro}$ was codon-optimized and synthesized (Tsingke Biotechnology Co., Ltd.), and subcloned into the pcDNA3.1 vector with a C-terminal FLAG-tag to produce the pcDNA3.1-$3CL^{pro}$-FLAG expression plasmid.

For construction of the linker mutant (Q/A), $3CL^{pro}$ G11A and $3CL^{pro}$ P132H mutant, the sites-directed mutagenesis was performed using QuickMutation™ Site-Directed Mutagenesis Kit (Beyotime) following the Manufacturer's instructions. All plasmid DNA constructs were sequenced.

Coelenterazine-h was purchased from Promega. Ebselen and all the inhibitors were purchased from Target Molecule and prepared in DMSO. DYKDDDDK (Flag) Tag antibody (8146) was purchased from Cell Signaling Technology, Inc (CST, USA), β-actin antibody (ab8224) from Abcam, HRP-conjugated goat anti-mouse secondary antibody (sc-2031) from Santa Cruz.

2.3. BRET assay

For BRET assay, transfected cells were seeded in 96 well white plates with clear bottom. After overnight incubation, DMSO (Sigma-Aldrich) or compounds were added to each well at the designated concentration. After a further incubation for 48 h at 37 °C, the supernatant was discarded. A stock of coelenterazine-h was dissolved in absolute ethyl alcohol to a concentration of 1.022 mmol/L. For luminescence assay, 100 μL of 10 μM coelenterazine-h was injected, and luminescence was measured using VICTORTM X5 2030 Multilable Reader (PerkinElmer).

2.4. Western blot

HEK293T cells were seeded at a density of 2×10^5 cells per well in 6-well plate. After overnight incubation, DMSO (Sigma-Aldrich) or compounds were added to each well at the designated concentration. After a further incubation for 48 h at 37 °C, transfected HEK293T cells were collected and lysed in RIPA buffer containing 50 mM Tris (pH 7.4), 150 mM NaCl, 1% NP-40, 0.1% SDS, 1 mM EDTA, 0.5% sodium deoxycholate. Cell lysates were mixed with SDS loading buffer and boiled for 20 min, followed by electrophoresis in 10% polyacrylamide-SDS gels. Proteins were transferred onto PVDF membrane. After blocking with 5% Skim milk, the membrane was blotted with anti-Flag (1:1000), or anti-β-actin (1:5000) antibodies. After incubation with HRP-conjugated secondary antibodies (1:5000), protein signals were detected with enhanced chemiluminescence.

2.5. Cell viability assay

Cell viability was performed by Cell Counting Kit-8 (CCK-8) (Beyotime, China). Typically, HEK293T cells were seeded in the wells of 96-well plate at 100 μL/well and grown for 24 h. Then 10 μL of CCK-8 reagent and incubated for 1.5 h at 37 °C with 5% CO2. The absorbance at 450 nm was subsequently measured using EnSpire 2300 Multilable Reader (PerkinElmer).

2.6. Microscale thermophoresis assay (MST)

The MST assays were conducted as previously described (Yang et al., 2020; Yao et al., 2019). To detect interactions between $3CL^{pro}$ and compounds, 3CL protein was labeled with the red fluorescent dye NHS according to the instructions of Monolith™ Series Protein Labeling Kit RED-NHS 2nd Generation (NanoTemper Technologies GmbH, Munich, Germany). The concentration of NHS-labeled 3CL was held constantly at 100 nM, whereas the concentrations of compounds were gradient-diluted (from 100 μM, 50 μM–25 μM, until 0.00305 μM). After brief incubation, the samples were loaded into MST-standard glass capillaries. The measurements were performed at 25 °C on a MST machine (NanoTemper Technologies, Munich, Germany).

2.7. Anti-coronavirus activity assay

The anti-coronavirus activity was measured by MTS Cell Proliferation Colorimetric Assay kits (Promega, Madison, WI, USA). Briefly, HCT-

8 cells were inoculated with HCoV-OC43 at a multiplicity of infection (MOI) of 0.1. After incubated in 2% FBS and each of test compounds for 120 h at 33 °C in 5% CO2 incubator, 20 mL of MTS Cell Proliferation Colorimetric reagent was added into each well and incubated for another 3 h at 37 °C. The absorbance at 490 nm was measured using the Enspire 2300 Multiable reader (PekinElmer).

2.8. Quantification and statistical analysis

Data are presented as mean ± standard deviation (SD) from at least three independent experiments unless otherwise indicated, and were analyzed with GraphPad Prism. Difference between the two indicated settings were considered statistically significant if $p < 0.05$(*), $p < 0.01$ (**), $p < 0.001$(***). n.s indicates nonsignificant.

3. Results

3.1. Establishing the cell-based BRET assay for SARS-CoV-2 3CL^{pro}

In order to develop a cell-based BRET assay suitable for rapid screening of SARS-CoV-2 3CL^{pro} inhibitor, we first constructed the expression vector pEYFP-linker-Rluc. The linker sequence (ITSAVLQSGFRK), which consists of 12 adjacent amino acids existing in the polyprotein of SARS-CoV and SARS-CoV-2, has been reported to be specifically recognized by 3CL^{pro} (Lee et al., 2014; Vatansever et al., 2021). Here, the linker was inserted in frame between pEYFP and Rluc to express the fusion protein pEYFP-linker-Rluc. The scheme of the assay was illustrated in Fig. 1A. Addition of Rluc substrate coelenterazine h induces Rluc emission at 475 nm, and initiates the resonance energy transfer to pEYFP and its emission at 535 nm in the case of a close distance between pEYFP and Rluc (<100 Å). When SARS-CoV-2 3CL^{pro} is expressed in the cells, it will cleave its substrate to distance the pEYFP and Rluc protein, and block the resonance energy transfer, thereby lowing the BRET ratio. Therefore, a BRET value quantitatively reflects the activity of 3CL^{pro}.

To verify that 3CL^{pro} was able to cleave efficiently the substrate pEYFP-linker-Rluc, 293T cells were co-transfected with fixed amount of plasmid expressing pEYFP-linker-Rluc and increasing amounts of plasmid expressing SARS-CoV-2 3CL^{pro}. The BRET and Western blot analysis showed that while there was no detectable cleavage of pEYFP-linker-Rluc fusion protein in empty vector transfected cells, the increasing expression of 3CL^{pro} protein enhanced pEYFP-linker-Rluc cleavage as indicated by the diminishing abundance of the pEYFP-linker-Rluc fusion protein, the dose-dependent accumulation of the pEYFP signals, and a gradual reduction in the BRET ratio (Fig. 1B), which showed a striking direct correlation between the cellular activity of SARS-CoV-2 3CL^{pro} and the BRET ratios.

Meanwhile, in order to determine the specificity of the cleavage, we constructed a linker mutant in the 3CL^{pro} substrate with mutation of Q to A, which has been reported to be a highly conservative cleavage position for 3CL^{pro} (Pablos et al., 2021; Shan and Xu, 2005). Wild-type and mutant substrates were separately coexpressed with 3CL^{pro}, and

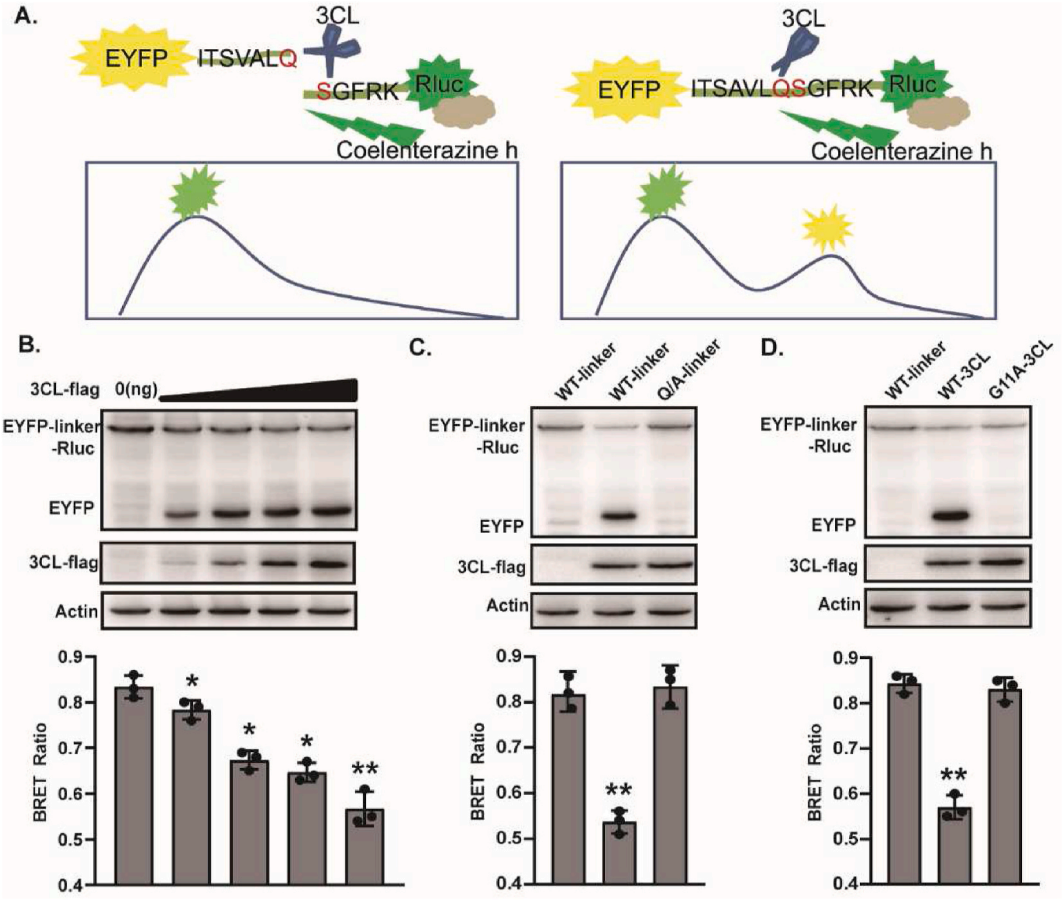

Fig. 1. Overview of the cell-based BRET screening assay. (A) Schematic representation of the BRET assay. (B) HEK293T cells (4×10^5) were co-transfected with 3CL-flag and EYFP-linker-Rluc plasmid DNA in different proportions. After 48 h post-transfection, cells were collected for Western blot and BRET ratio analysis. (C) The Q/A-linker mutant could not be cleaved efficiently by 3CL. HEK293T cells were transfected with 3CL-flag and EYFP-linker-Rluc (or Q/A-linker mutant) plasmid DNA. After 48 h post-transfection, cells were collected for Western blot and BRET ratio analysis. (D) The G11A 3CL mutant disables cleaving activity. HEK293T cells were transfected with 3CL-flag (G11A 3CL mutant) and EYFP-linker-Rluc plasmid DNA. After 48 h post-transfection, cells were collected for Western blot and BRET ratio analysis. All the results shown are the average of three independent experiments. (*P < 0.05; **P < 0.01).

cleavage of pEYFP-linker-Rluc fusion protein was analyzed by Western blot and the activity of 3CL^{pro} was evaluated by measuring BRET signal, which were corrected for nonspecific background value, as measured from the cells transiently expressing unfused EYFP and Rluc. As shown in Fig. 1C, the BRET ratio significantly reduced with the cleavage of the wild-type substrate to yield more EYFP protein by the 3CL^{pro}, whereas 3CL^{pro} failed to induce efficient cleavage of the mutant substrate, with no obvious change in the BRET ratio. Furthermore, 3CL^{pro} G11A mutant has been reported to fail to function by disrupting its dimerization (Chen et al., 2008; Goyal and Goyal, 2020), thus we also determined the effect of the wild-type and G11A mutant 3CL^{pro} on the cleavage of pEYFP-linker-Rluc substrate. Western blot showed that wild-type 3CL^{pro}, but not G11A mutant, induced the efficient cleavage of pEYFP-linker-Rluc fusion protein. Likewise, the results of BRET assay were consistent with that of Western blot (Fig. 1D). The results suggested that the 3CL^{pro} can efficiently and specifically cleave the substrate pEYFP-linker-Rluc, and correspondingly, induce the changes of BRET value.

3.2. Screening of known HIV/HCV protease inhibitors against SARS-CoV-2 3CL^{pro} using the BRET assay

These data above suggest that the BRET assay is highly specific and sensitive, making it a promising tool for screening of SARS-CoV-2 3CL^{pro} inhibitors in live cells. The FDA approved SARS-CoV-2 3CL^{pro} inhibitor nirmatrelvir was used as a positive control to validate availability of the BRET assay. The result showed that nirmatrelvir effectively inhibited the 3CL^{pro} activity with an EC_{50} value of 1.45 μM (Fig. S1), which is in corroborate with the previous study showing its antiviral activity against SARS-CoV-2 with EC_{50} value of 77.9 nM in A549-ACE2 and 61.8 nM in dNHBE cells (Owen et al., 2021). To evaluate its feasibility in HTS assay, we performed the BRET assay under optimized conditions with sample wells transfected with 3CL^{pro} as the positive control and empty vector-transfected wells as the negative control. The assay showed a Z′-factor of 0.59, a coefficient of variation (CV) of 3.98%, and the signal-to-noise (S/N) ratio of 10.95, all of which met the requirement for HTS assay (Table 1). Taken together, these data demonstrate that the cell-based BRET assay is suitable for HTS for SARS-CoV-2 3CL^{pro} inhibitors.

We then performed the screen with a collection of protease inhibitors using the BRET assay, which were selected from Target Molecule lnc. To experimentally evaluate for inhibitory activity against SARS-CoV-2 3CL^{pro}. The primary screening of the 26 known HIV or HCV protease inhibitors (Table 2) was conducted at a final concentration of 20 μM. We use ebselen as the positive control, which has been reported to strongly inhibit 3CL^{pro} activity with an EC_{50} of 0.67 μM (Jin et al., 2020) and DMSO-treated cell wells were served as intraplate negative control for data normalization. At least triplicate repeats were performed for each tested compound and the control. Initial hits were defined as those active compounds that displayed the BRET ratio with significant difference, compared with that of the control group. The results presented in Fig. 2 showed that 9 inhibitors, met the hit criteria in the screen. In contrast, little or no inhibition activity against SARS-CoV-2 3CL^{pro} was detected in the BRET assay with other tested compounds at 20 μM concentration level. Among the hits, nelfinavir mesylate, saquinavir, bevirimat, and nelfinavir are HIV protease inhibitors, and telaprevir, asunaprevir, simeprevir, grazoprevir and dasabuvir are HCV protease inhibitors.

Table 1
Summary of statistical parameters to assess the robustness of the HTS assay.

Statistical parameters	Value
Z'[a]	0.59
S/N[c]	10.95
%CV[b]	3.98

[a] $Z' = 1–3(STD_{3CL+\ cells} + STD_{3CL-\ cells})/(MEAN_{3CL+\ cells}\text{-}MEAN_{3CL-\ cells})$.
[b] %CV(coefficient of variation) = $STD_{3CL+\ cells}/MEAN_{3CL+\ cells}X100\%$.
[c] S/N(signal-to-noise ratio) = $(Mean_{3CL\ +\ cells}\text{-}Mean_{3CL-\ cells})/((STD_{3CL+\ cells})^2+(STD_{3CL-\ cells})^2)^{1/2}$.

Table 2
List of protease inhibitors tested against SARS-CoV-2 3CL protease in the BRET assay.

Name	CAS	Target
Atazanavir sulfate	229975-97-7	HIV Protease inhibitor
Atazanavir	198904-31-3	HIV Protease inhibitor
Ritonavir	155213-67-5	HIV Protease inhibitor
Lopinavir	192725-17-0	HIV Protease inhibitor
Des(benzylpyridyl) Atazanavir	1192224-24-0	HIV Protease inhibitor
Darunavir	206361-99-1	HIV Protease inhibitor
Limonin	1180-71-8	HIV Protease inhibitor
Darunavir Ethanolate	635728-49-3	HIV Protease inhibitor
Nelfinavir Mesylate	159989-65-8	HIV Protease inhibitor
Amprenavir	161814-49-9	HIV Protease inhibitor
saquinavir	127779-20-8	HIV Protease inhibitor
indinavir	157810-81-6	HIV Protease inhibitor
Fosamprenavir calcium salt	226700-81-8	HIV Protease inhibitor
Bevirimat	174022-42-5	HIV Protease inhibitor
Nelfinavir	159989-64-7	HIV Protease inhibitor
Paritaprevir	1221573-85-8	HCV Protease inhibitor
HZ1157	1009734-33-1	HCV Protease inhibitor
Danoprevir	850876-88-9	HCV Protease inhibitor
Telaprevir	402957-28-2	HCV Protease inhibitor
Asunaprevir	630420-16-5	HCV Protease inhibitor
Simeprevir	923604-59-5	HCV Protease inhibitor
Boceprevir	394730-60-0	HCV Protease inhibitor
Glecaprevir	1365970-03-1	HCV Protease inhibitor
4-Phenoxybenzylamine	107622-80-0	HCV Protease inhibitor
Grazoprevir	1350514-68-9	HCV Protease inhibitor
Dasabuvir(ABT-333)	1132935-63-7	HCV Protease inhibitor

3.3. Determining the 3CL^{pro} inhibitory activity of hits using the BRET assay

To further demonstrate the availability of the cell-based BRET assay for SARS-CoV-2 3CL^{pro} inhibitors screening, we characterized the inhibitory activities of these hits against SARS-CoV-2 3CL^{pro}. Dose-response experiments were performed to determine their EC_{50} values by varying the compound concentrations from 20 nM to 100 μM. 293T cells were transfected with plasmids expressing pEYFP-linker-Rluc and SARS-CoV-2 3CL^{pro} before treatment with increasing doses of inhibitors. The BRET values were then measured and the inhibitory rates were calculated for inhibitor treatments compared to DMSO control, which were then plotted as dose-response curves for determining the inhibitor efficacies EC_{50} values. We collectively presented the results in Fig. 3A and observed a gradual decrease in cleavage efficacy of 3CL^{pro} under the treatment of all the 9 compounds. Eight compounds exhibited strong inhibitory activity, with EC_{50} values of 0.8–21 μM, while saquinavir had less potent 3CL^{pro} inhibitory activity, with an EC_{50} value of 40 μM.

Meanwhile, to rule out that such EC_{50} values of these compounds were stemmed from their cytotoxicity, we also evaluated the cellular cytotoxicity of these hits using CCK-8 assay. 293T cells were treated with DMSO or different concentrations of hits up to 200 μM, and cell viability was plotted to calculate the 50% cell cytotoxicity (CC_{50}) values. We found that eight of these hits showed well acceptable cellular cytotoxicity, with CC_{50}s ≥ 100 μM. Only dasabuvir showed the slightly higher cytotoxicity, with CC_{50} value of 70 μM (Fig. 3B). Together, these data support the utility of this cell-based assay in screening for SARS-CoV-2 3CL^{pro} inhibitors.

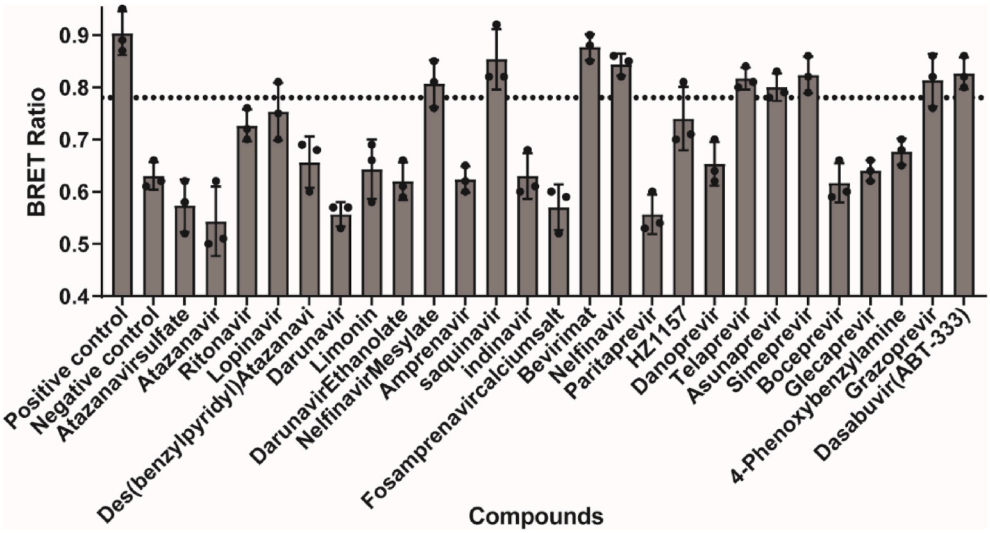

Fig. 2. Results of the high-throughput screening. (A) HEK293T cells were co-transfected with 3CL-flag and EYFP-linker-Rluc plasmid DNA at the ratio of 5:1. At 12 h post-transfection, the cells were re-seeded in 96-well plates (10^4/well) and treated with all the inhibitors at the concentration of 20 μM. After 36 h, BRET ratio was measured. All data are expressed as mean ± SD of triplicate assays.

3.4. The antiviral activity of hits against human coronavirus strains HCoV-OC43

Like SARS-CoV-2, HCoV-OC43 also belongs to beta CoVs, and shares 47% sequence identity in $3CL^{pro}$ from SARS-CoV-2, both of which shows highly structural similarity in catalytic domain (Fig. S2). Thus, we assessed the antiviral activities of these hits against HCoV-OC43 instead of SARS-CoV-2. A cell-based MTS assay was performed using HCT-8 cell lines infected with HCoV-OC43, followed by treated with serial dilutions of hits, and then their antiviral activities were evaluated by measuring cell viability against CoV-induced cytopathic effect (CPE). As shown in Fig. 4, all hits exhibited a dose-dependent inhibitory effect on the replication of HCoV-OC43 strain, and seven of the compounds showed EC_{50} values of 10 μM–50 μM, while bevirimat and grazoprevir did not significantly inhibit OC43 infection even at the high concentration of 50 μM. The results suggest that most of the hits can inhibit HCoV-OC43 strain but exhibit weaker potency against HCoV-OC43, compared with SARS-CoV-2 $3CL^{pro}$.

3.5. Binding of hits to SARS-CoV-2 $3CL^{pro}$

To test whether SARS-CoV-2 $3CL^{pro}$ is the direct target for these hits, we then performed microscale thermophoresis (MST) assay to assess the binding capacity of these hits to SARS-CoV-2 $3CL^{pro}$ *in vitro*, in expect of exploring the possible mechanism of action of hits against SARS-CoV-2 $3CL^{pro}$. The labeled SARS-CoV-2 $3CL^{pro}$ (100 nM) was incubated with hits at different serially diluted concentrations from 0.0153 μM to 500 μM, which were then loaded into premium capillaries and measured by using 40% MST power. As shown in Fig. 5, four of the 9 compounds were identified to exhibit concentration response curves of binding with SARS-CoV-2 $3CL^{pro}$. The dissociation constants (Kd) of hits were determined and listed in Table 3. One of the hits, simeprevir, presented the strongest binding affinity to SARS-CoV-2 $3CL^{pro}$ with a Kd value of 2.10 μM. Bevirimat exhibited a moderate binding to SARS-CoV-2 $3CL^{pro}$ with a Kd value of 10.50 μM, Compounds nelfinavir and telaprevir bound weakly to SARS-CoV-2 $3CL^{pro}$, with higher Kd values of 91.62 μM and 62.95 μM, respectively.

3.6. Binding model

To shed more light on these interactions, we also computed the structure of $3CL^{pro}$ of SARS-CoV-2 in complex with these compounds. As shown in Table 4, the four compounds have binding energy values between −6.7 and −8.2 kcal/mol. Consistent with the result of MST assay, compound simeprevir was predicted to bind to SARS-CoV-2 $3CL^{pro}$ with the most favorable binding energy (ΔG_{ADV} = -8.2 kcal/mol). To explore the binding mode of identified inhibitors, molecular docking study of simeprevir against SARS-CoV-2 $3CL^{pro}$ (PDB-ID: 6XQS) was performed by AutoDock Vina. As shown in Fig. 6, simeprevir is located in the active site pocket of SARS-CoV-2 $3CL^{pro}$. Specifically, simeprevir forms hydrogen bond with E166. In addition, the compound showed hydrophobic interaction with L27, V42, C44, M49, P52, Y54, C145, M165, L167, P168, and A191.Polar interactions were also observed between simeprevir and T24, T25, T26, H41, N142, H164, Q189, T190, and Q192. These interactions occurred between simeprevir and the essential amino acids at the binding pocket, especially H41 and C145, suggesting that simeprevir may block the entry of the substrate toward the catalytic cleft of $3CL^{pro}$. Taken together, the data suggest the direct interaction between the hits and SARS-CoV-2 $3CL^{pro}$, and further demonstrate the availability of the established cell-based BRET assay for SARS-CoV-2 $3CL^{pro}$ inhibitors screening.

Currently, five 'variants of concern' (VOC) have been identified (Alpha, Beta, Gamma, Delta and Omicron). Although the spike (S) glycoprotein appears especially prone to accumulate mutations, two amino acid changes in $3CL^{pro}$ were also described, which include K90R in Beta and P132H in Omicron, respectively. Based on the predicted binding model, these mutations most unlikely affect the binding of simeprevir to $3CL^{pro}$, therefore no difference in susceptibility for simeprevir is expected. In line with it, we found a similar effect of simeprevir on cleavage efficiency of $3CL^{pro}$ containing these two mutations, compared with that of ancestral virus (Fig. 7). This not only further supports the predicted binding model, but also suggests the potential of simeprevir for the treatment of the SARS-CoV-2 variants infection.

4. Discussion

COVID-19 pandemic has brought great damage to both public health and the global economy. Although significant progress has been made in the development of effective vaccines, there is still an urgent need to discover effective targeted therapeutics for SARS-CoV-2 infection, particularly in light of the rapid emergency of variant strains. It is reported that SARS-CoV-2 $3CL^{pro}$ is highly conserved and the extremely low mutation rate on its binding domain will not broadly impact the efficacy of SARS-CoV-2 $3CL^{pro}$ inhibitors (Gao et al., 2021). In this study,

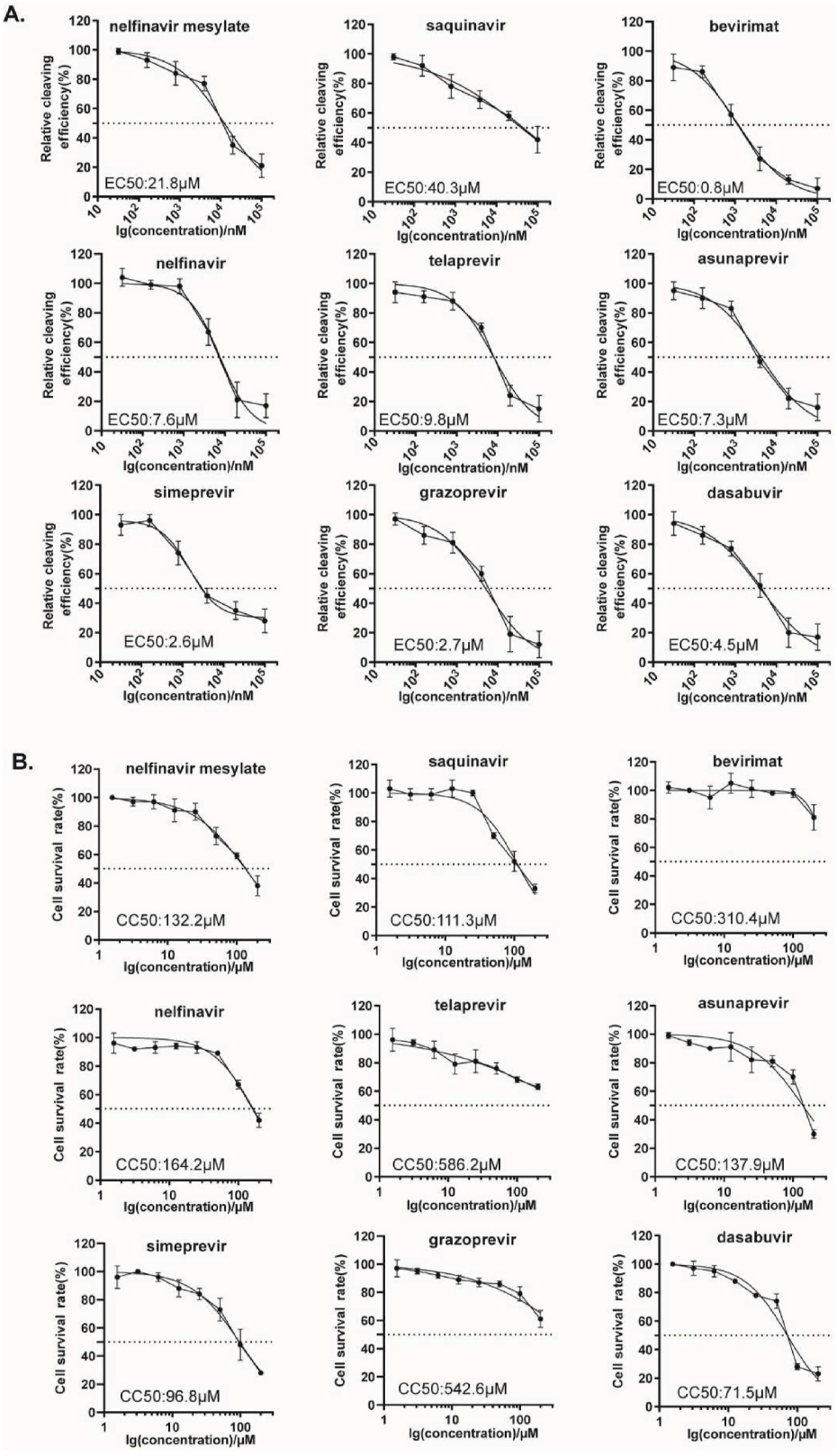

Fig. 3. Dose-response inhibition curves of selected hits against $3CL^{pro}$. (A) HEK293T cells were co-transfected with 3CL-flag and EYFP-linker-Rluc plasmid DNA at the ratio of 5:1. At 12 h post-transfection, the cells were re-seeded in 96-well plates (10^4/well) and treated with serially diluted compounds. After 36 h, BRET ratio was measured. (B) CC_{50} values in the cells were measured using CCK-8 kits. All data are expressed as mean ± SD of triplicate assays.

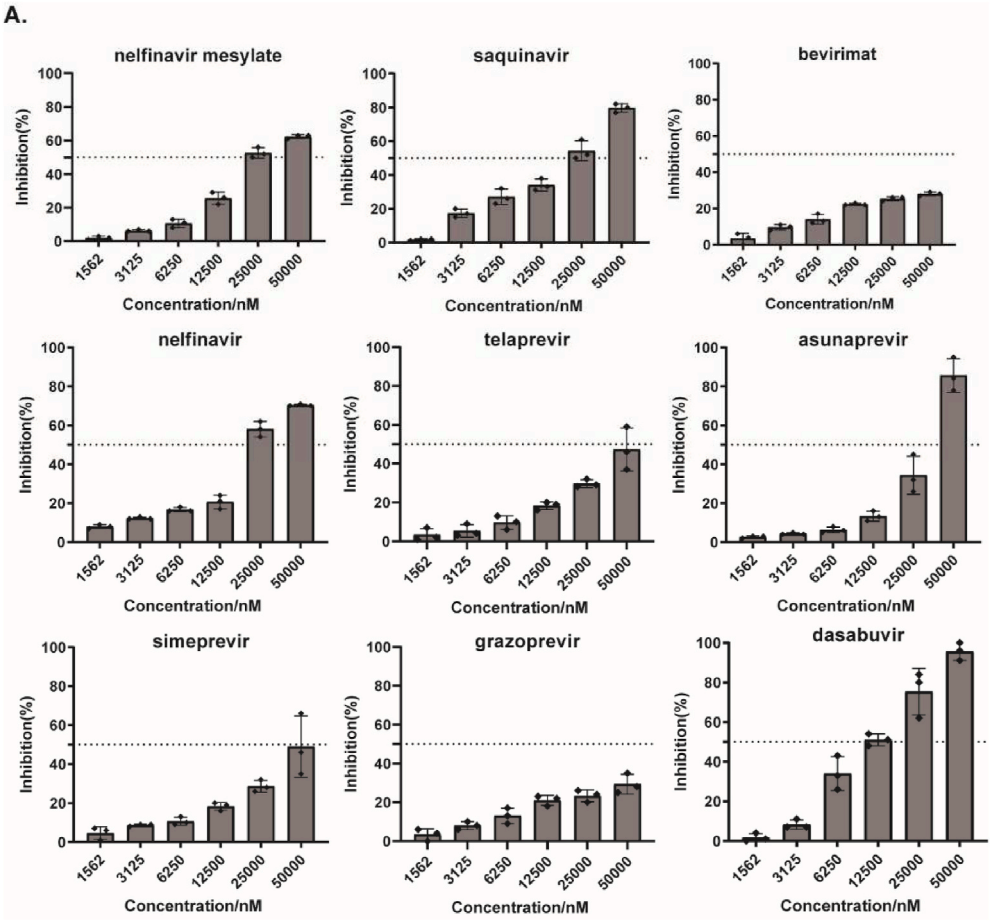

Fig. 4. Evaluation of antiviral activity of the hits against human coronavirus strains HCoV-OC43. HCT-8 cells were infected by HCoV-OC43 at a MOI (multiplicity of infection) of 0.1, and treated with serial dilutions of each hit. The effect of the treatments on cell viability was measured via MTS assay at 120 h post-infection.

we established a cell-based BRET assay for screening inhibitor targeting SARS-CoV-2 $3CL^{pro}$ (Fig. 1). The assay could be performed without the need of a high-level biosafety laboratory environment and is available for the high-throughput screening. Compared with the cell-free FRET assay, the cell-based assay closely mimicked the viral-infected cells, thus the result is in general well-correlated with the antiviral activity. Furthermore, cell-based assay will exclude cytotoxic or membrane impermeable compounds, which may be hits in the cell-free assays. Several cell-based SARS-CoV-2 $3CL^{pro}$ inhibition assays have been reported including the FlipGFP assay (Li et al., 2021; Ma et al., 2022), the Protease-Glo luciferase assay (Mathieu et al., 2021), and the cell cytotoxicity assay (Cao et al., 2022). Considering the fluorescence signals are acquired by imaging and flow cytometry in the FlipGFP assay and the cell cytotoxicity assay, the BRET assay has superior advantages of a straight-forward ratiometric calculation by measuring luminescence after a simple addition of a substrate, and lower background signals almost without autofluorescence. However, it is for this reason that the signal is usually weaker in the BRET assay than that in these other cell-based assays.

Using the optimized and validated BRET assay, we screened a collection of HIV/HCV protease inhibitors (Table 2 and Fig. 2) and nine compounds were selected as potential inhibitors of $3CL^{pro}$. Furthermore, our data of their $3CL^{pro}$ inhibitory activities (Fig. 3) and binding affinities with $3CL^{pro}$ (Fig. 5 and Table 4) showed that of the nine screened hits, simeprevir was identified as the most potent inhibitors. Simeprevir, a HCV NS3/4A protease inhibitor, is one of FDA-approved prescription drugs used in the treatment of HCV infection (Zhang, 2016). In our assay, simeprevir was determined to efficiently inhibit SARS-CoV-2 $3CL^{pro}$ activity with an EC_{50} value of 2.6 μM in 293T cells, which is almost line with previous studies that displayed potent antiviral activities of simeprevir against SARS-CoV-2. Simeprevir had been reported to inhibit SARS-CoV-2 replication with an EC_{50} of 1.41–15 μM in Vero E6, 9 μM in A549-hACE2 and 14 μM in Huh7.5 cells (Gammeltoft et al., 2021; Lo et al., 2021; Muturi et al., 2022), and EC_{50} of 2.3 μM in 293T-ACE2 cells (Bafna et al., 2021). Thus, together with that of our assay, simeprevir was demonstrated to effectively inhibit SARS-CoV-2 virus replication in cell lines.

In addition, we proposed several other compounds as potential inhibitor candidates of SARS-CoV-2 $3CL^{pro}$. In fact, some of these HCV protease inhibitors have also been explored as SARS-CoV-2 $3CL^{pro}$ inhibitors by other groups (Gammeltoft et al., 2021; Bafna et al., 2021; Ma et al., 2020; Kneller et al., 2020). Their antiviral activities have also been approved in Vero E6 or 293T cells, such as grazoprevir, asunaprevir, telaprevir (Bafna et al., 2021), dasabuvir (Hayashi et al., 2021). Although our results were roughly consistent with these previous findings, some of these compounds reportedly active against SARS-CoV-2, such as paritaprevir and boceprevir (Bafna et al., 2021; Ma et al., 2020), did not exert inhibitory activity based on our BRET assay. Moreover, nelfinavir mesylate was also screened out to inhibit SARS-CoV-2 $3CL^{pro}$ activity herein, and was reported to directly inhibit S-mediated cell fusion (Musarrat et al., 2020). Thus, the discrepancy may be due to different cell types or multitarget activity of inhibitors. In our study, four of the 9 candidates with cellular activity were identified to bind with SARS-CoV-2 $3CL^{pro}$ *in vitro* (Fig. 5). The discrepancies between the results from cell-based assay and the *in vitro* binding assay could be attributed to that some compounds inhibit the activity of SARS-CoV-2 $3CL^{pro}$ indirectly. Furthermore, it is worth to mention that these different conclusions suggest that the BRET screening assay still

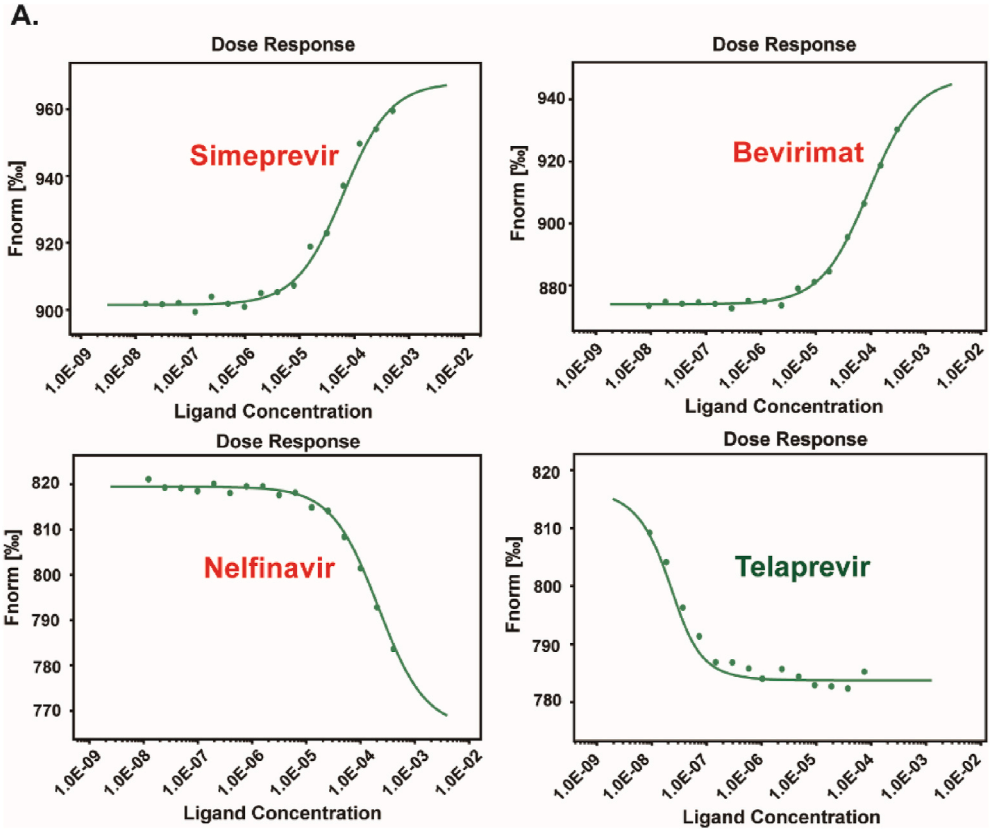

Fig. 5. MST assays for the binding of the hits to $3CL^{pro}$ protein *in vitro*. All the hits at different serially diluted concentrations (0.0153 μM–500 μM) were titrated into a fixed concentration of labeled $3CL^{pro}$ protein (100 nM). The detailed dataset was shown in the table.

Table 3
Summary of the detailed dataset and of the MST assay.

Target name:	3CL			
Target concentration:	100 nM			
Ligand name:	Simeprevir	Bevirimat	Nelfinavir	Telaprevir
Ligand Concentration:	0.0153 μM–500 μM			
MST Power:	40%			
Kd(M):	2.0988E-06	1.0496E-05	9.1615E-05	6.2951E-05
Kd confidence:	±4.5051E-06	±8.7665E-06	±7.6979E-05	±1.6454E-05
Signal to Noise	17.54	20.25	78.69	16.70

Table 4
The molecule name (MolName),CAS, calculated binding energies($\triangle G_{ADV}$, kcal/mol) of compounds.

No.	MolName	CAS	$\triangle G_{ADV}$
1	Bevirimat	174022-42-5	−6.7
2	Nelfinavir	159989-64-7	−7.8
3	Telaprevir	402957-28-2	−7.0
4	Opt_Simeprevir	923604-59-5	−8.2

has some limitations and further improvements are needed to evaluate the proposed drug candidates.

The recent rises of several high transmissible variants including Delta and Omicron strains of SARS-CoV-2 sounded alarms for currently used prevention and therapeutic tools. Interestingly, we found that simeprevir showed the most potency against $3CL^{pro}$ with an EC_{50} vale of 2.6 μM, and a similar activity against the protease containing the mutation derived from the current virus strain. This suggests the potential of simeprevir for the treatment of the SARS-CoV-2 variants infection. Omicron $3CL^{pro}$ harbors a P132H mutation and several groups have reported that P132H $3CL^{pro}$ and wild-type $3CL^{pro}$ exhibited comparable enzymatic properties for its substrate (Ullrich et al., 2022; Greasley et al., 2022; Sacco et al., 2022). The crystal structures of P132H $3CL^{pro}$ in complex with nirmatrelvir or GC-376 have been solved and show that P132H mutation does not induce any significant structural changes and backbone conformational shift from wildtype $3CL^{pro}$ (Greasley et al., 2022; Sacco et al., 2022), which may explain why Omicron $3CL^{pro}$ lacks the resistance to simeprevir. Never the less, we found that most of the hits exhibit weaker potency against HCoV-OC43 with higher EC_{50} values, compared with that of SARS-CoV-2 $3CL^{pro}$. We aligned the sequences of HCoV OC43 $3CL^{pro}$ (YP_009555250.1) and SARS-CoV-2 $3CL^{pro}$ using the multiple sequence alignment tool CLUSTALW (Fig. S2). The amino acid sequence of $3CL^{pro}$ protein of HCoV OC43 shows 47% similarity to that of SARS-CoV-2. This may partly explain the difference in inhibitory activities of these hits between HCoV-OC43 and SARS-CoV-2 $3CL^{pro}$.

In summary, we have developed and evaluated a high throughput cell-based BRET assay for screening of SARS-CoV-2 $3CL^{pro}$ protease inhibitors. Even though cell lines could not entirely reflect *in vivo* situations, and future detailed validation studies are required to fully define the potential inhibitors for COVID-19 treatments, this work provides a robust model to better discover pre-*in vivo* antivirals.

Funding

This work was supported by CAMS Innovation Fund for Medical Sciences [2021-I2M-1–038, 2022-I2M-JB-014 and 2021-I2M-1–055]; the National Natural Science Foundation of China [81903679, 81971950]; and Fundamental Research Funds for the Central Universities [3332021045].

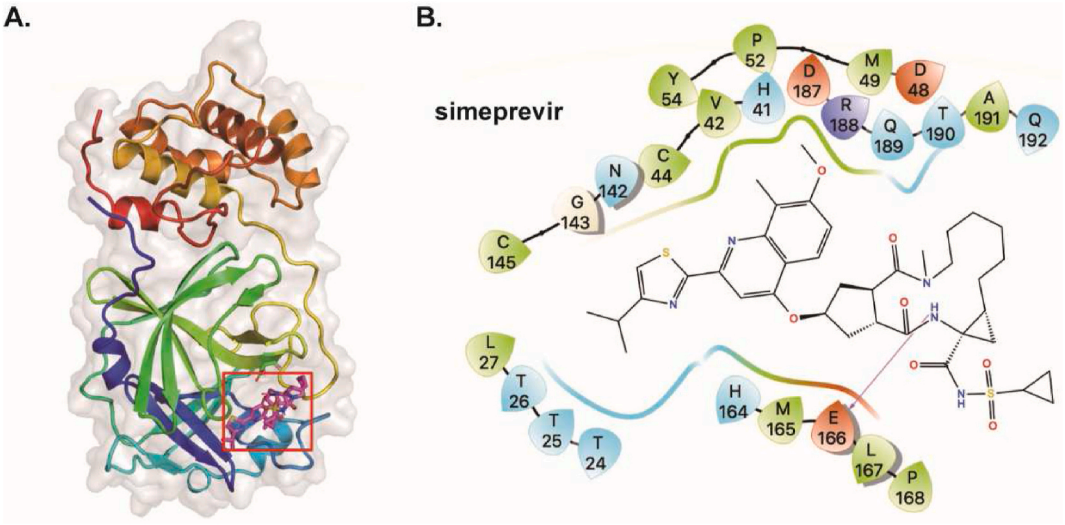

Fig. 6. Binding pose analysis of simeprevir. (A) Predicted structure of SARS-CoV-2 $3CL^{pro}$ in complex with simeprevir (B) Residues within 5 Å of simeprevir are shown on the 2D ligand interaction diagram. For clarity, only polar hydrogen atoms were shown. Here the color code is that dark blue is positively charged, red is negatively charged, cyan is polar, green is hydrophobic. Hydrogen bonding was depicted as magenta arrows.

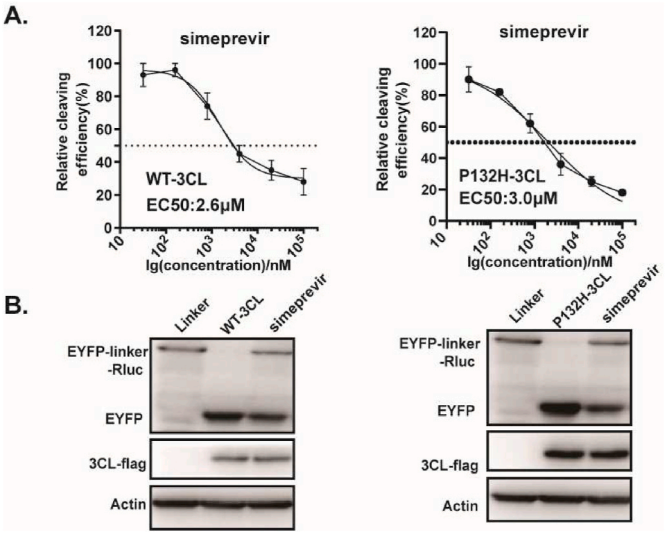

Fig. 7. Effect of simeprevir on 3CL Omicron variants. (A) HEK293T cells were co-transfected with 3CL-flag (WT or P132H 3CL mutant) and EYFP-linker-Rluc plasmid DNA. At 12 h post-transfection, the cells were re-seeded in 96-well plates (10^4/well) and treated with serially diluted simeprevir. After 36 h, BRET ratio was measured. (B) HEK293T cells (4×10^5) were co-transfected with 3CL-flag (WT or P132H 3CL mutant) and EYFP-linker-Rluc plasmid DNA. At 12 h post-transfection, the cells were treated with simeprevir (20 μM). After 48 h post-transfection, cells were collected for Western blot. All the results shown are the average of three independent experiments.

Author contributions

S.C., L.Y. and J.W. designed the study; L.M., Q.L. and Y.X. performed the main part of the experimental study; D.Y., S.G. contributed to data analysis; F.G. contributed Key reagents; J.W. drafted the paper; S.C. and L.Y. revised the manuscript. All authors analyzed the results and approved the final version of the manuscript.

Declaration of competing interest

The authors declare that they have no known competing financial interests or personal relationships that could have appeared to influence the work reported in this paper.

Acknowledgments

We thank National Infrastructure of Microbial Resources (NIMR-2014-3, China) and CAMS Collection Center of Pathogenic Microorganisms (CAMS-CCPM-A, China) for providing valuable reagents.

Appendix A. Supplementary data

Supplementary data to this article can be found online at https://doi.org/10.1016/j.antiviral.2022.105419.

References

Ahmad, B., Batool, M., Ain, Q.U., et al., 2021 Aug 24. Exploring the binding mechanism of PF-07321332 SARS-CoV-2 protease inhibitor through molecular dynamics and binding free energy simulations. Int. J. Mol. Sci. 22 (17).

Bafna, K., White, K., Harish, B., et al., 2021 May 18. Hepatitis C virus drugs that inhibit SARS-CoV-2 papain-like protease synergize with remdesivir to suppress viral replication in cell culture. Cell Rep. 35 (7), 109133.

BioRender. COVID-19 vaccine & therapeutics tracker. Available from: https://biorender.com/covid-vaccine-tracker/.

Cannalire, R., Cerchia, C., Beccari, A.R., et al., 2020 Nov 13. Targeting SARS-CoV-2 proteases and polymerase for COVID-19 treatment: state of the art and future opportunities. J. Med. Chem. 65 (4), 2716–2746.

Cao, B., Wang, Y., Wen, D., et al., 2020 May 7. A trial of lopinavir-ritonavir in adults hospitalized with severe covid-19. N. Engl. J. Med. 382 (19), 1787–1799.

Cao, W., Cho, C.D., Geng, Z.Z., et al., 2022 Feb 23. Evaluation of SARS-CoV-2 main protease inhibitors using a novel cell-based assay. ACS Cent. Sci. 8 (2), 192–204.

Chen, S., Hu, T., Zhang, J., et al., 2008 Jan 4. Mutation of Gly-11 on the dimer interface results in the complete crystallographic dimer dissociation of severe acute respiratory syndrome coronavirus 3C-like protease: crystal structure with molecular dynamics simulations. J. Biol. Chem. 283 (1), 554–564.

Dai, W., Zhang, B., Su, H., et al., 2020 Apr 22. Structure-based design of antiviral drug candidates targeting the SARS-CoV-2 main protease. Science 368 (6497), 1331–1335.

FDA US. Coronavirus disease 2019 emergency use authorization information. Available from: https://www.fda.gov/emergency-preparedness-and-response/mcm-legal-regulatory-andpolicy-framework/emergency-use-authorization#coviddrugs.

Gammeltoft, K.A., Zhou, Y., Duarte Hernandez, C.R., et al., 2021 Aug 17. Hepatitis C virus protease inhibitors show differential efficacy and interactions with remdesivir for treatment of SARS-CoV-2 in vitro. Antimicrob. Agents Chemother. 65 (9), e0268020.

Gao, K., Wang, R., Chen, J., et al., 2021 Nov 19. Perspectives on SARS-CoV-2 main protease inhibitors. J. Med. Chem. 64 (23), 16922–16955.

Goyal, B., Goyal, D., 2020 Jun 8. Targeting the dimerization of the main protease of coronaviruses: a potential broad-spectrum therapeutic strategy. ACS Comb. Sci. 22 (6), 297–305.

Greasley, S.E., Noell, S., Plotnikova, O., et al., 2022 Jun. Structural basis for the in vitro efficacy of nirmatrelvir against SARS-CoV-2 variants. J. Biol. Chem. 298 (6), 101972.
Hayashi, T., Murakami, K., Hirano, J., et al., 2021 Dec 22. Dasabuvir inhibits human norovirus infection in human intestinal enteroids. mSphere 6 (6), e0062321.
Islam, R., Parves, M.R., Paul, A.S., et al., 2020 May 12. A molecular modeling approach to identify effective antiviral phytochemicals against the main protease of SARS-CoV-2. J. Biomol. Struct. Dyn. 1–12.
Jin, Z., Du, X., Xu, Y., et al., 2020 Jun. Structure of M(pro) from SARS-CoV-2 and discovery of its inhibitors. Nature 582 (7811), 289–293.
Kandeel, M., Al-Nazawi, M., 2020 Jun 15. Virtual screening and repurposing of FDA approved drugs against COVID-19 main protease. Life Sci. 251, 117627.
Khan, S.A., Zia, K., Ashraf, S., et al., 2020 Apr 13. Identification of chymotrypsin-like protease inhibitors of SARS-CoV-2 via integrated computational approach. J. Biomol. Struct. Dyn. 1–10.
Kneller, D.W., Galanie, S., Phillips, G., et al., 2020 Dec 1. Malleability of the SARS-CoV-2 3CL M(pro) active-site cavity facilitates binding of clinical antivirals. Structure 28 (12), 1313–1320 e3.
Lee, W., Kim, S.J., 2022 Jul 19. Current updates on COVID-19 vaccines and therapeutics: as of june 2022. Biotechnol. Bioproc. Eng. 1–7.
Lee, H., Mittal, A., Patel, K., et al., 2014 Jan 1. Identification of novel drug scaffolds for inhibition of SARS-CoV 3-Chymotrypsin-like protease using virtual and high-throughput screenings. Bioorg. Med. Chem. 22 (1), 167–177.
Li, X., Lidsky, P.V., Xiao, Y., et al., 2021 Sep. Ethacridine inhibits SARS-CoV-2 by inactivating viral particles. PLoS Pathog. 17 (9), e1009898.
Lo, H.S., Hui, K.P.Y., Lai, H.M., et al., 2021 May 26. Simeprevir potently suppresses SARS-CoV-2 replication and synergizes with remdesivir. ACS Cent. Sci. 7 (5), 792–802.
Lobo-Galo, N., Terrazas-Lopez, M., Martinez-Martinez, A., et al., 2020 May 14. FDA-approved thiol-reacting drugs that potentially bind into the SARS-CoV-2 main protease, essential for viral replication. J. Biomol. Struct. Dyn. 1–9.
Ma, C., Sacco, M.D., Hurst, B., et al., 2020 Aug. Boceprevir, GC-376, and calpain inhibitors II, XII inhibit SARS-CoV-2 viral replication by targeting the viral main protease. Cell Res. 30 (8), 678–692.
Ma, C., Tan, H., Choza, J., et al., 2022 Apr. Validation and invalidation of SARS-CoV-2 main protease inhibitors using the Flip-GFP and Protease-Glo luciferase assays. Acta Pharm. Sin. B 12 (4), 1636–1651.
Mathieu, C., Touret, F., Jacquemin, C., et al., 2021 Sep 12. A bioluminescent 3CL(pro) activity assay to monitor SARS-CoV-2 replication and identify inhibitors. Viruses 13 (9).
Mengist, H.M., Fan, X., Jin, T., 2020 May 9. Designing of improved drugs for COVID-19: crystal structure of SARS-CoV-2 main protease M(pro). Signal Transduct. Targeted Ther. 5 (1), 67.
Mirza, M.U., Froeyen, M., 2020 Aug. Structural elucidation of SARS-CoV-2 vital proteins: computational methods reveal potential drug candidates against main protease, Nsp12 polymerase and Nsp13 helicase. J Pharm Anal 10 (4), 320–328.
Musarrat, F., Chouljenko, V., Dahal, A., et al., 2020 Oct. The anti-HIV drug nelfinavir mesylate (Viracept) is a potent inhibitor of cell fusion caused by the SARSCoV-2 spike (S) glycoprotein warranting further evaluation as an antiviral against COVID-19 infections. J. Med. Virol. 92 (10), 2087–2095.
Muturi, E., Hong, W., Li, J., et al., 2022 Jan. Effects of simeprevir on the replication of SARS-CoV-2 in vitro and in transgenic hACE2 mice. Int. J. Antimicrob. Agents 59 (1), 106499.
Nutho, B., Mahalapbutr, P., Hengphasatporn, K., et al., 2020 May 12. Why are lopinavir and ritonavir effective against the newly emerged coronavirus 2019? Atomistic insights into the inhibitory mechanisms. Biochemistry 59 (18), 1769–1779.
Owen, D.R., Allerton, C.M.N., Anderson, A.S., et al., 2021 Dec 24. An oral SARS-CoV-2 M (pro) inhibitor clinical candidate for the treatment of COVID-19. Science 374 (6575), 1586–1593.
Pablos, I., Machado, Y., de Jesus, H.C.R., et al., 2021 Oct 26. Mechanistic insights into COVID-19 by global analysis of the SARS-CoV-2 3CL(pro) substrate degradome. Cell Rep. 37 (4), 109892.
Sacco, M.D., Hu, Y., Gongora, M.V., et al., 2022 May. The P132H mutation in the main protease of Omicron SARS-CoV-2 decreases thermal stability without compromising catalysis or small-molecule drug inhibition. Cell Res. 32 (5), 498–500.
Sciscent, B.Y., Eisele, C.D., Ho, L., et al., 2021. COVID-19 reinfection: the role of natural immunity, vaccines, and variants. J. Community Hosp. Intern. Med. Perspect. 11 (6), 733–739.
Shan, Y.F., Xu, G.J., 2005 Dec. Study on substrate specificity at subsites for severe acute respiratory syndrome coronavirus 3CL protease. Acta Biochim. Biophys. Sin. 37 (12), 807–813.
Sk, M.F., Roy, R., Jonniya, N.A., et al., 2020 May 12. Elucidating biophysical basis of binding of inhibitors to SARS-CoV-2 main protease by using molecular dynamics simulations and free energy calculations. J. Biomol. Struct. Dyn. 1–21.
Ton, A.T., Gentile, F., Hsing, M., et al., 2020 Mar 11. Rapid identification of potential inhibitors of SARS-CoV-2 main protease by deep docking of 1.3 billion compounds. Mol Inform 39 (8), e2000028.
Ullrich, S., Ekanayake, K.B., Otting, G., et al., 2022 Apr 15. Main protease mutants of SARS-CoV-2 variants remain susceptible to nirmatrelvir. Bioorg. Med. Chem. Lett. 62, 128629.
Vatansever, E.C., Yang, K., Drelich, A.K., et al., 2021 Mar 9. Bepridil is potent against SARS-CoV-2 in Vitro. Proc. Natl. Acad. Sci. U. S. A. 118 (10), e2012201118.
Yang, K.S., Leeuwon, S.Z., Xu, S., et al., 2022 Jul 14. Evolutionary and structural insights about potential SARS-CoV-2 evasion of nirmatrelvir. J. Med. Chem. 65 (13), 8686–8698.
Zhang, X., 2016 Jan. Direct anti-HCV agents. Acta Pharm. Sin. B 6 (1), 26–31.
Zhang, L., Lin, D., Sun, X., et al., 2020 Apr 24. Crystal structure of SARS-CoV-2 main protease provides a basis for design of improved alpha-ketoamide inhibitors. Science 368 (6489), 409–412.